Exact quantum calculations of the kinetic isotope effect: Cross sections and rate constants for the F+HD reaction and role of tunneling

Dario De Fazio,[a] Vincenzo Aquilanti, and Simonetta Cavalli
Dipartimento di Chimica, Università di Perugia, 06123 Perugia, Italy

Antonio Aguilar and Josep M. Lucas
Departamento de Quimica Fisica, Universitat de Barcelona, 08028 Barcelona, Spain

(Received 9 May 2006; accepted 15 June 2006; published online 3 October 2006)

In this paper we present integral cross sections (in the 5–220 meV collision energy range) and rate constants (in the 100–300 K range of temperature) for the F+HD reaction leading to HF+D and DF+H. The exact quantum reactive scattering calculations were carried out using the hyperquantization algorithm on an improved potential energy surface which incorporates the effects of open shell and fine structure of the fluorine atom in the entrance channel. The results reproduce satisfactorily molecular beam scattering experiments as well as chemical kinetics data for both the HF and DF channels. In particular, the agreement of the rate coefficients and the vibrational branching ratios with experimental measurements is improved with respect to previous studies. At thermal and subthermal energies, the rates are greatly influenced by tunneling through the reaction barrier. Therefore exchange of deuterium is shown to be penalized with respect to exchange of hydrogen, and the isotopic branching exhibits a strong dependence on translational energy. Also, it is found that rotational excitation of the reactant HD molecule enhances the production of HF and decreases the reactivity at the D end, obtaining insight on the reaction stereodynamics. © *2006 American Institute of Physics*. [DOI: 10.1063/1.2221695]

I. INTRODUCTION

In the last two decades since the crossed molecular beam study in Lee's laboratory,[1] the reaction of the fluorine atom with molecular hydrogen has offered an unprecedented opportunity for comparing reaction rate information obtained from quantum mechanical reactive scattering calculations with experimental measurements.[2]

Besides its relevance for chemical lasers, this reaction has played a very important role in the development of exact and approximate methodologies to study the chemical reactivity at the most detailed level, and nowadays it is used as a textbook example of elementary chemical reactions. Recently several studies (Refs. 2 and 3 and references therein) have provided a detailed understanding of how electronic structure governs chemical reactivity in the gas phase by establishing a bridge between the potential energy surface and the kinetic observables, such as cross sections (the most detailed quantities measured in molecular beam experiments and obtainable from first-principles calculations of reactive collisions) and rate constants, of prime importance for chemical kinetics and its applications.[3]

In this paper, we focus our attention on the isotopic variant, the F+HD reaction, which offers us the unique occasion to tackle by exact quantum dynamics the basic problem of the energy and temperature dependence of the intermolecular kinetic isotope effect for the branching ratio of the reaction leading to the products HF or DF. Already since the 1985 experimental study, again from Lee's laboratory,[4] the F+HD reaction was suggested to be the isotopic variant of the $F+H_2$ family exhibiting the largest quantum effects. This was argued on the basis of simple kinematic arguments. A three-dimensional quantum reactive scattering calculation for this reaction at the energies of this experiment was performed only 13 years later,[5] and stronger evidence of quantum mechanical effects was observed lowering the collision energies.[6] In this latter work a clear resonance around 0.52 kcal/mol was documented by a molecular beam experiment as well as in quantum calculations on the potential energy surface (PES) of Ref. 7 [Stark and Werner (SW) PES in the following]. Further experimental studies[8,9] in the low collision energy range have shown an interesting role of this resonance also on state-to-state observables, such as rotational selected differential cross sections and rotational product distributions. Such rotational selected fingerprint of resonance behavior is another important distinguishing feature with respect to the $F+H_2$ isotopic variant.[10]

This feature of the F+HD reaction is also very attractive from a more fundamental point of view, because it has been shown[11] that it provides an ideal setting for an extensive quantum control in chemical reactions, namely, the ability through laboratory parameters to completely suppress or maximally enhance a particular arrangement channel by manipulating quantum interference contributions. Previous theoretical results,[6] although in only qualitative agreement with experiment with respect to the shape and position of the steplike resonance behavior, overestimate its height by a factor as large as 2: it remains unclear whether the reason of this disagreement arose from the neglect of possible contribu-

[a]Author to whom correspondence should be addressed; also at Istituto di Metodologie Inorganiche e dei Plasmi-C.N.R., 70126 Bari, Italy; electronic mail: dario@dyn.unipg.it

tions of nonadiabatic effects in the entrance channel or from known minor inaccuracies of the PES in the exit channel region.[5] Concerning rate constants, time dependent close coupling calculations[12] indicated the need of further work regarding the isotopic ratio and this using both SW PES and a more recent one,[13] which incorporated the role of open-shell and spin-orbit effects. All these calculations were carried out adiabatically, i.e., on a single PES.

Extensive studies of nonadiabatic effects in the dynamics of $F+H_2$ reaction[14] demonstrated that their role was small, but the inclusion of the fine structure splitting appeared to lead to an increase in the reaction barrier giving a smaller reactivity with respect to the experimentally measured values. However, subsequent nonadiabatic calculations performed on the F+HD system both by time dependent[15,16] and time independent approaches[17] have shown that the open-shell structure of the fluorine atom has a stronger influence on F+HD than it does on the $F+H_2$ isotopic variant. Comparison with the experiments suggested that an adjustment of the energy scale was required in order to reproduce the energy position of the resonance feature.

Relativistic effects, such as the spin-orbit interaction of the open-shell F atom in the entrance channel, are very hard to be treated with *ab initio* approaches, so that uncertainties are to be expected in these PESs. A few years ago we have suggested[18] a new ground adiabatic PES taking into account of open-shell and spin-orbit effects by a description of the entrance channel long range behavior[19] as obtained from elastic scattering measurements[20] of magnetically selected F atoms. In this PES, called PES III in Ref. 3, the long range entrance channel region was merged to the SW PES in a way so to leave unmodified the energy of the transition state. A near perfect agreement with measured rate constants[21] was obtained for the $F+H_2$ reaction at temperatures between 200 and 335 K showing the key role of our corrections especially in the cold condition regime. Spin-orbit effects are expected to be even more important for the F+HD variant. Moreover, since new measured rate constants[22] of the two separated exit channels are now available in a lower temperature range, reactive calculations of the F+HD isotopic variant is a crucial test of the accuracy of our PES III. The extensive exact time independent quantum dynamical calculations were made possible by a computer code which implements our *hyperquantization algorithm*.[23]

Quantum reactive scattering calculations on potential energy surfaces provide state-to-state differential and integral cross sections as well as rate constants for both channels of the reaction of fluorine atoms with HD molecules. In this paper, we focus on reaction integral cross sections and rate constants. Results are found to reproduce satisfactorily experimental data for the two channels,[6,22] validating the PES III description of the reaction entrance channel. Comparison with experimental results will provide further insights on improvements on the potential surface, particularly in the exit channel. In Sec. II, we describe briefly the hyperquantization algorithm. The main results are presented and discussed in Sec. III. Conclusions are given in Sec. IV.

II. THEORETICAL AND COMPUTATIONAL DETAILS

Quantum mechanical calculations of reaction dynamics are carried out using the hyperquantization algorithm amply described in Refs. 23 and 24. This exact treatment of an elementary chemical reaction as a quantum mechanical three body problem has been applied also to the study of the prototypical ion-molecule reaction $He+H_2^+ \rightarrow HeH^+ + H$.[25] Within the framework of the hyperspherical coordinates approach to reaction dynamics, we solve the Schrödinger equation at fixed values of the hyper-radius ρ using the discrete analogs of hyperspherical harmonics as basis functions. The eigenvalues as a function of the hyperradial variable define the effective potentials employed in the propagation step for the solution of the multichannel reactive scattering problem. The discrete analogs of hyperspherical harmonics are orthogonal polynomials of a discrete variable, closely related to the vector coupling coefficients of angular momentum theory.[26] The kinetic energy is represented in this basis, and the potential is diagonal on a grid on the hypersphere—a feature similar to discrete variable representations.

This time independent close coupling method generates, for a specific energy E, total angular momentum J and for each value of the inversion parity, the entire scattering matrix $\mathbf{S}^J(E)$, whose square modulus elements are state-to-state reaction probabilities. The total integral cross section as a function of the relative translational energy of reactants, $\sigma(E)$, is obtained as follows:

$$\sigma(E) = \sum_{nn'} f_n \sigma_{nn'}(E). \tag{1}$$

Here, f_n is the fraction of the total number of collisions that occur with the colliding particles in the initial state denoted by n and $\sigma_{nn'}$, which are state-to-state integral cross sections,

$$\sigma_{nn'}(E) = \frac{\pi\hbar^2}{4\mu E} \sum_J \frac{2J+1}{g_n} |S^J_{nn'}(E)|^2, \tag{2}$$

where μ is the reduced mass of the reactants, g_n is the initial state degeneracy factor, and the square modulus of the scattering matrix elements $|S^J_{nn'}|^2$ are reaction probabilities from the reactant state n to the final product state n'. Rate constants are calculated summing state-to-state reaction probabilities over initial and final states accessible to the system at a given energy and averaging over the Maxwell-Boltzmann distribution of the initial translational energy. The bimolecular rate constant k as function of temperature T is given by

$$k(T) = \left(\frac{2}{RT}\right)^{3/2} \frac{1}{(\pi\mu)^{1/2}} \int_0^\infty E\sigma(E) e^{-E/RT} dE, \tag{3}$$

with R being the gas constant.

Four projections Ω (helicities) on the least inertia principal axis of the total angular momentum J were taken into account in the calculations. The truncation error introduced by this choice was less than 0.5% for the total integral cross sections with initial $j \leqslant 3$. However, for $j=4$ this error increases and therefore we do not use j values higher than 3 in the summations giving rate constants. The number of the

TABLE I. Numerical parameters for the production runs of the hyperquantization algorithm.

ρ (a_0)	I	N	e_{cut} (eV)	n_{cut}	D
		Truncation on Φ_ν			
2.2	1500	108		24	36 024
3	1500	108		44	66 064
4	1500	108		69	103 569
		Truncation on Θ_τ			
5	2900	116	30.0	54	4653
6	4500	144	18.5	37	3329
7	5800	168	8.0	22	1777
8	6900	192	6.8	19	1505
9	8000	220	5.6	17	1261
10	9000	244	5.5	16	1217
11	9900	272	5.4	16	1208
12	10800	300	5.4	16	1215

calculated adiabatic states are 350, 336, 322, and 308 for $\Omega=0$, 1, 2, and 3, respectively. Convergence tests were made on the $J=0$ reaction probabilities. The maximum values of the vibrational quantum number in the asymptotic channels corresponding to this choice were 1, 4, and 6 for HD, HF, and DF, respectively. The remaining parameters required in the propagation step have been taken as in Ref. 18 for the $F+H_2$ reaction. The maximum number of total coupled channels propagated was 1316 for total angular momentum larger than 4. Since this is the first application of our algorithm to an A+BC asymmetric system, we have checked carefully the accuracy of our implementation comparing differential and integral cross sections using SW PES with those that we obtained running the ABC code[28] at selected collision energies. A very satisfactory agreement was recorded at the same level published in Ref. 18 for the H_2 isotopic variant.

Input parameters for the hyperquantization algorithm used in the production runs are given in Table I as a function of the hyper-radius ρ. The meaning of these parameters and the convergence criterion has been given in Refs. 24 and 27 and will not be repeated here. In the first and second columns, values I and N of total grid points for the hyperangles Θ and Φ, respectively,[23] are listed. In the last column we report the dimension D of the Hamiltonian matrix for $\Omega=0$ resulting from the reduction according to the sequential diagonalization scheme described in Ref. 27. These numbers can be taken as an indication of the computational effort required for the calculation of the adiabatic eigenfunctions with our method. However, it is important to note that the structure of the matrices is different for the values of ρ smaller and larger than $4.6a_0$, for which two alternative sequential diagonalization schemes were adopted.[27] In particular, the Hamiltonian matrix is full above this ρ value [where a $V_{max}=2.9$ eV (Ref. 24) was used], while it is block tridiagonal in the region of strong interaction. Therefore, in spite of the larger matrix dimensions at small ρ, the use of the diagonalization method for sparse matrices based on the Lanczos algorithm permits a faster solution. The largest computational effort is therefore in the intermediate ρ region at the border of the range of application of the two diagonalization-truncation schemes.

We computed the scattering matrix at 60 energies in the collision energy range from 5 to 270 meV relative to the ground rotovibrational state of HD. The adopted energy grid was of 1 meV in the resonance region and of 5 meV elsewhere. In order to generate fully convergent cross sections, values of total angular momentum J up to 35 (up to 21 for the lower limit of the energy range) had to be used. Rate constants were convergent within 1% with respect to these parameters. Initial rotational states until $j=3$ are used in the rate constants averaging. Since in the experiment $j=4$ is about 2% (Ref. 29) of the total HD at the higher temperature considered in this work, on the basis of calculations performed at selected energies with $\Omega_{max}=5$ (see above), we can estimate a maximum error due to this choice of about 2%–3% for the HF channel and less than 1% for DF. The different sensitivity of the two reactive channels is due to the different dependence of the reactivity with the reactants' rotational energy, as will be documented in the next section. In the range of temperatures between 200 and 300 K this is the largest source of error in our calculations and it establishes confidence range of the values of our rate constants.

III. DISCUSSION AND RESULTS

The dynamical calculations employ a potential energy surface referred to as PES III in Ref. 3 (available in Ref. 30). Figure 1 shows schematically salient aspects of the potential energy surface profile. Particularly under focus is the presence of a potential well that leads to a van der Waals complex in the entrance channel which is an important feature of many reactions,[31] specifically of $F+H_2$.[10,32] PES III incorporates the correct entrance channel behavior [19] as known from scattering experiments of magnetically selected fluorine atoms by hydrogen molecules.[20] For reference and comparison with previous work,[6] we also performed calculations on the SW PES.[7] PES III has transition state features very similar to the SW PES, but with respect to the latter the van der Waals entrance channel well is slightly shallower and occurs on at larger reactants' distance, and the barrier width is slightly thicker on account of the spin-orbit interaction effects on the electronically adiabatic lowest surface.[18,19] In Refs. 3 and 18,

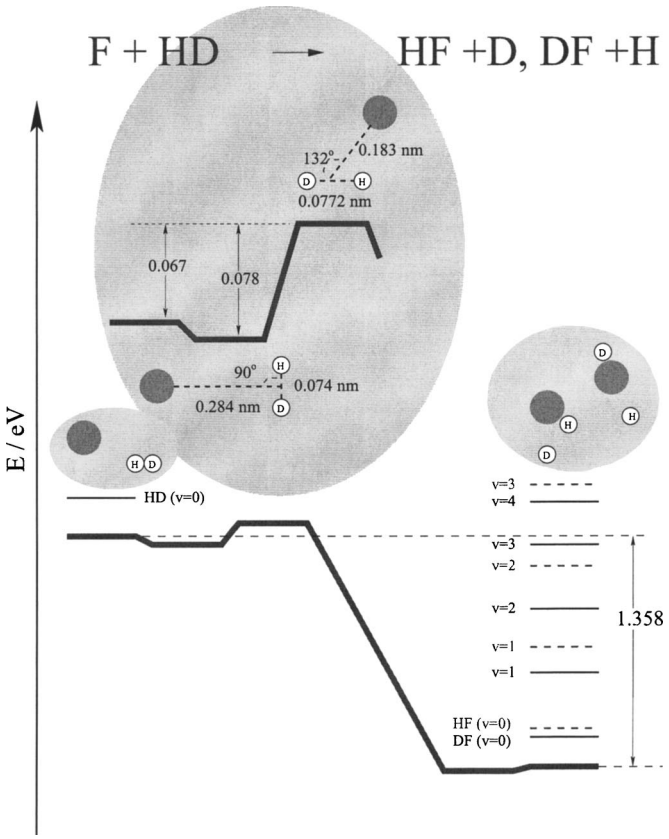

FIG. 1. Schematic profile of the geometry and energetics of the channels for reactants and products, and for the transition state for the F+HD (v=0) reaction giving D+HF or H+DF. In the collision energy range considered, HD is in its v=0 vibrational state. It is shown that vibrational states for HF up to v=3 and for HD up to v=4 can be populated. The large ellipse shows the entrance channel van der Waals well and the transition state features for the present potential energy surface, PES III. The exit channel van der Waals well occurs in a collinear configuration with a depth similar to that of the entrance channel.

PES III was found able to satisfactorily account for several known facts about the $F+H_2$ reaction, including the rate constant values.

A. Integral cross sections

For this reaction, the isotopic branching ratio depends strongly on the translational energy and on the reactant rotational quantum number. Here we show in Fig. 2 the cross sections for selected initial j=0, 1, 2, and 3 rotational states of HD, summed over all energetically permitted rotational final states of the HF and DF (Fig. 1) molecules. Such information is required to obtain, by an extension of Eq. (1), converged rotational averaged rate constants (see Ref. 3 for numerical details of the calculation) below and near room temperature. We note that the initial rotational energy has an opposite effect on the reactivity of two product channels. This emerged also in previous calculations.[12] In particular, the rotational energy increases the reactivity at the H end and decreases the DF reactivity. However, larger effects can be observed for HF than for DF, where the reactivity of j=3 at 60 meV of collision energy is more than three times that of j=0. Moreover such an effect increases with j, while decreases in the DF case.

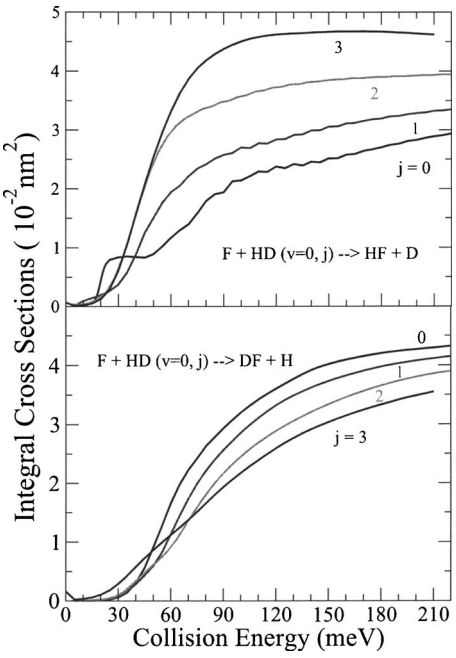

FIG. 2. Calculated cross sections for PES III for rotationally selected initial state (j=0, 1, 2, and 3) as a function of collision energy.

In Fig. 3 the behavior of the isotopic branching ratio of cross sections Γ (DF/HF) as a function of the collision energy is shown for the different rotational reactant quantum numbers j for both SW and PES III. In all cases, except for j=3 for the PES III surface, Γ (DF/HF) dramatically decreases at collision energies lower than the barrier height (see Fig. 1). This is expected: at low collision energies the tunneling effect favors H exchange. On the contrary at higher energies, the asymmetry of the center of mass of the HD molecule offers a wider acceptance cone at the D end favoring the reactivity to DF. The effect of the initial rotational energies on the branching is consistent with kinematic considerations within the classical mechanics framework:[33] in fact, since the center of mass of HD is closer to the D end, the rotational motion leads to a screening of the D atom by the faster rotating H atom that hinders approach of trajectories to the transition state from the D end.

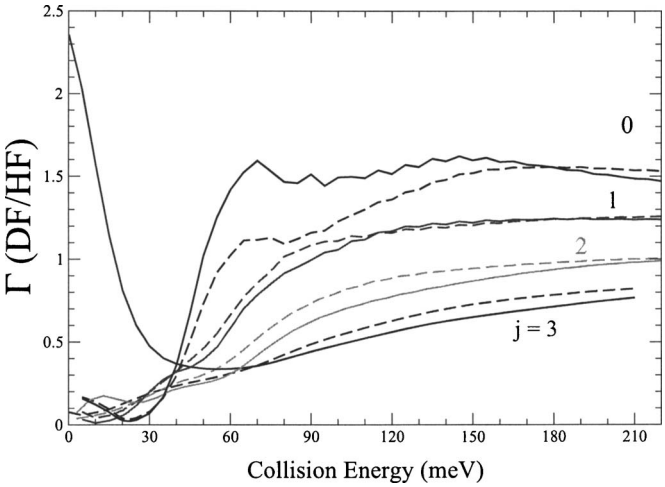

FIG. 3. Isotopic branching ratios for PES III (solid lines) and SW PES (dashed lines) for rotationally selected initial state (j=0, 1, 2, and 3) as a function of collision energy.

In Fig. 3, we can observe that SW and PES III results have similar behavior. However, the $j=3$ case is an interesting exception where low energy reactivity strongly favors the DF product. This is a marked stereodynamical effect for PES III, presumably related to the specific geometry of its van der Waals entrance channel well. An analysis in terms of the effect of helicities Ω on the cross sections (not presented here) shows that the increase of the isotopic branching ratio is mainly due to the highest Ω values. This behavior is particularly evident for j larger than 3. In the asymptotic region where the well is located, Ω (which is the projection of the total angular momentum J along the least inertia axis of the principal axis frame) tends to coincide with the projection of the rotational angular momentum j of HD along the atom-molecule direction **R**. It is known (and our exact calculations confirm) that Ω is a nearly conserved quantity for this reaction. In the vector model in the limit of large j, the highest value of the j projection corresponds to the reactant molecule rotating in a plane perpendicular to **R**, enabling an insertion mechanism to reaction, favored by the van der Waals attractive forces in the entrance channel. These effects will be stronger at low collision energy, specifically for PES III where the van der Waals well is located at larger distances than for the SW PES. The insertion mechanism increases the yield of DF because the transition state from the D end has a larger Jacobi (attack) angle,[33] being the molecular center of mass closer to the D atom than to H. However, to fully understand such an effect, a stereodirected analysis should be done by an approach similar to the one used in Ref. 34 for the $F+H_2$ case.

For comparison with experimental cross section data,[6] the information for $j=0$ and 1 is combined to give the integral cross sections shown in the upper panel of Fig. 4. In the lower panel SW PES results are also reported. Since only relative values are experimentally given, a proper normalization is required. In the upper panel of Fig. 4 the normalization factor is taken to optimize the overall agreement between PES III calculations and experiments. It is only ~5% higher from the normalization factor used in the lower panel where essentially the same factor of Ref. 6 has been used. The overall agreement was found satisfactory in previous work using the SW PES,[6] although the theory yields a resonance feature around 23 meV of collision energy, slightly shifted and much more pronounced than observed in the experiments. Such a discrepancy is attenuated, but not fully eliminated by our PES III. In particular, the intensity of the resonance peak clearly agrees better with the experimental findings, but it is not so for its location, which remains nearly unchanged with respect to SW PES case. This is not surprising, being known[6] that this resonance complex is localized in the exit channel near to the transition state region, which is the same in both PESs. Also it can be noted that the experimental results show a fluctuating structure in the high and medium energy ranges that is not reproduced by calculations. Computed integral cross sections have some oscillating behavior, but it is less pronounced than the experimental one.

In Fig. 5 product vibrationally selected integral cross sections for all the open channels of the two reactive channels calculated on the PES III are compared with experimental measurements.[35] The agreement is remarkable for all the reactive channels of both reactions, except for $v'=3$ of HF where a large and wide bimodal peak is completely missed

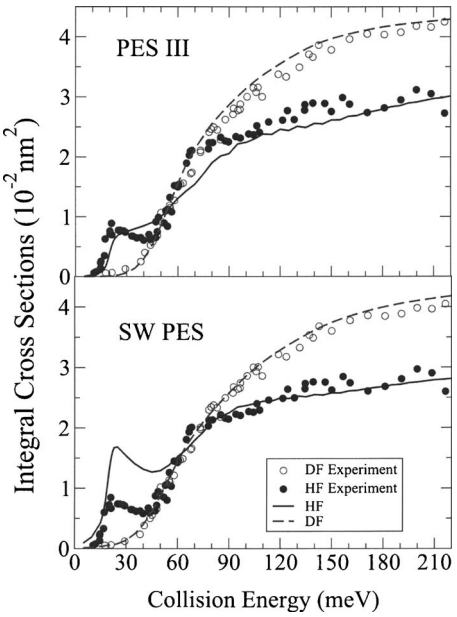

FIG. 4. Integral cross sections calculated in comparison with the experimental results of Ref. 6 (full and open dots for the HF and DF channels). They are obtained by taking contributions of the state selected cross section of Fig. 2 from $j=0$ and $j=1$, which are experimentally given as 82% and 18%, respectively. Experiments do not provide absolute values, but only relative ones so a normalization is required for comparison. Those for the two PES differ slightly (less than 5%). Our results for the SW surface agree with those of Ref. 6 within a few percent. The present calculations extend the energy range beyond 180 meV.

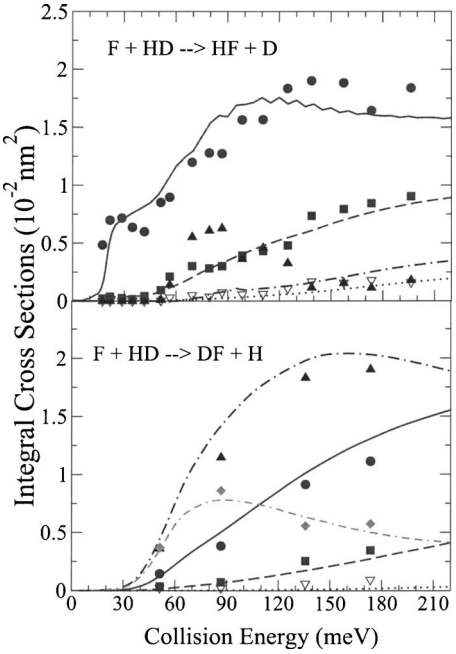

FIG. 5. Cross sections for production of HF ($v'=1$, 2, and 3: upper panel) and DF ($v'=1$, 2, 3, and 4: lower panel) in specific vibrational states. Symbols: experiments (Ref. 35); curves: present calculations (PES III). $v'=0$, open triangles and dots; $v'=1$, full squares and dashes; $v'=2$, full dots and continuous curves; $v'=3$, full triangles and dashed-dot curves; $v'=4$, diamonds and double-dash-dot curves.

from the theory. Comparison of Fig. 5 with the upper panel of Fig. 4 shows clearly that most of the larger differences between experiment and theory can be attributed to a poor description of the dynamics of the $v'=3$ channel of HF. These differences are not attenuated by the improvements of PES III over the SW PES in the description of the entrance channel. However, by analogy with the $F+H_2$ system,[10,32] we argue that the $v'=3$ HF product channel is mainly populated by Feshbach resonance decay located in the van der Waals exit channel region, so we conjecture that the origin of these discrepancies comes from deficiencies of the potential energy surface in the exit region.

Comparison with experiments reported in the upper panel of Fig. 4, shows only slightly better agreement than those of Fig. 5 in Ref. 17, where nonadiabatic reactive calculations on Alexander, Stark, and Werner (ASW) PES (Ref. 14) were performed. However, this agreement further validates the reliability of PES III in describing the open-shell effects on the reaction dynamics. Moreover, in our case the comparison with experimental results has been performed with no recourse to any energy scaling of the experiment. The quality of the agreement with vibrationally resolved integral cross section shown in Fig. 5 is clearly higher than that in the corresponding figures of Ref. 17, suggesting that the entrance channel description of PES III is more accurate than the *ab initio* one used in that paper. This is true especially for the $v'=2$ DF channel but also for the other reaction channels ($v'=1$ was not shown in Ref. 17). However, nonadiabatic reactive calculations show a slightly higher reactivity in $v'=3$ than for our calculations, but still at variance with the experimental behavior. Although the resonance energy region is well described in both calculations, we do not expect the same agreement in the rate constant branching ratio. In fact the rate constants obtained in Ref. 12 on the Hartke, Stark, and Werner (HSW) PES (Ref. 13) (a potential energy surface very similar to the ground state adiabatic PES that can be obtained by the ASW diabatic set) failed to give the improved agreement with experiments achieved in this paper.

B. Rate constants

Integrating $\sigma(E)$ on a very fine energy grid we can finally generate rate constants $k(T)$ (Fig. 6). A very recent paper[22] (see also Refs. 12 and 29) reconsidered existing experimental information on the branching ratio for the two channels, and reports new measurements of their sum giving the absolute values for both isotopic channels in the 193–300 K temperature range. Figure 6 shows our results for both SW and PES III on an Arrhenius plot. No normalization is involved here: it is thus demonstrated that PES III and the exact quantum mechanical dynamics of this paper generate quantitative agreement for the rate constants for the two reaction channels of this reaction. Concerning the mechanism for the kinetic isotopic effects, our results confirm previous analysis based on classical mechanics arguments,[33] such as the role of center-of-mass shift for the rotational energy dependence, illustrated in Fig. 3 and already discussed in Sec. III A.

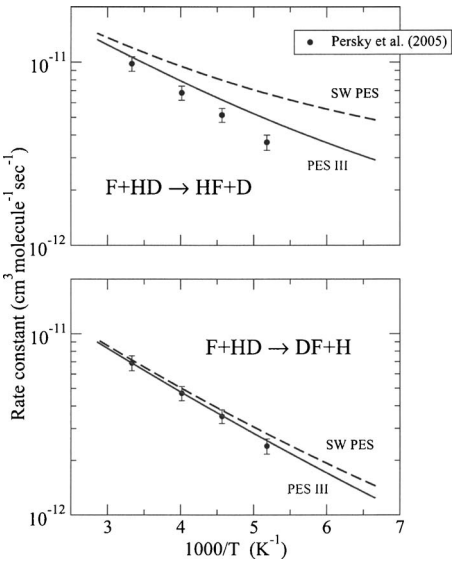

FIG. 6. Arrhenius plot (logarithm of rate constants vs inverse temperature) for the F+HD reaction. Dots: experimental data from Persky (2005) (Ref. 22); full lines: PES III (present calculations); dashed lines: SW (present calculations). Upper panel: the HF+D channel; lower panel: the DF+H channel.

As established in our previous work,[3] at room temperature and below the rates for this reaction are strongly influenced by tunneling. Figure 6 exhibits how penalized is deuterium with respect to hydrogen: this is due to higher mass and also to the higher zero point energy at the transition state (Fig. 1). Very interesting is the decrease in HF production when reactivity is considered on the PES III with respect to that on the SW potential energy surface. The thicker barrier of the PES III dramatically decreases tunneling improving agreement with experiment. Other information recently available[8,9] on differential cross sections and product rotational distributions is currently being processed according to our detailed quantum reactive scattering calculations to further assess the reliability of PES III, and specifically to indicate how to finely tune it to also improve the description of the exit channel.

Numerical tables on a fine grid are available on request from the authors. Tables II and III list values at temperatures relevant for comparison with experiments[22] and with previous close coupling time dependent calculations.[12] The level of agreement with both sets of data is impressive for the DF channel where all the given digits are exactly the same in the two SW calculations and inside the experimental error bars. For the HF production reaction, the differences between theoretical rates are slightly larger (between 1% and 4%, see Table III). These differences are within the estimated confidence error of this work in the range between 200 and 300 K where, as we have described in Sec. II, the effect of $j=4$ neglected in our calculation but not in Ref. 12 is expected to be of this order of magnitude for the HF product. Nevertheless in the range of 100–200 K the accuracy of our calculation is within 1% and we cannot attribute the apparent slight differences to this effect.

TABLE II. Comparison between experimental and theoretical rate constants (in cm^3 $molecule^{-1}$ $s^{-1} \times 10^{-12}$) for the F+HD→HF(DF)+D(H) reaction as a function of temperature.

	k_{HF+D}			k_{DF+H}		
T (K)	SW[a]	PES III[a]	Expt.[b]	SW[a]	PES III[a]	Expt.[b]
193	6.74	4.86	3.65±0.35	2.81	2.57	2.40±0.23
219	7.98	6.23	5.15±0.45	3.78	3.54	3.50±0.30
249	9.46	7.85	6.80±0.60	5.00	4.74	4.70±0.42
300	11.99	10.65	9.80±0.90	7.17	6.90	6.90±0.65

[a]Present work.
[b]Reference 22.

IV. CONCLUSIONS

In this paper we have presented results from a complete theoretical study of the chemical dynamics and kinetics of the F+HD reaction. Calculations are in a satisfactory agreement with experimental data.

Studying the motions of individual atoms as they interact during a reactive encounter, we have provided an explanation of the dramatic isotopic effect, observed experimentally, by making explicit reference to specific features of the potential energy surface. We have shown how the weak van der Waals interactions in the reactants' channel and tunneling through the potential barrier influence macroscopic observables, such as rate coefficients and vibrational branching ratios. These results validate the reliability of the potential energy surface used in the calculations, which has been obtained by blending the *ab initio* description of the transition state with a characterization of the long range potentials incorporating experimental information from the Perugia laboratory.[20] The inclusion of the latter is one of the key factors responsible of the improved agreement of the rate coefficients and the vibrational branching ratios with experimental measurements. The dependence of the intermolecular kinetic isotope effect on translational energy, rotational excitation, and tunneling through the reaction barrier has also been discussed.

Let us indicate directions along which further work is needed. The main point to be clarified is the production of HF in the $v'=3$ state, underestimated by the theory. In ample studies of resonance features for the $F+H_2$ reaction,[10,32] it has been concluded that, although PES III satisfactorily accounts for most of the observables which depend on the entrance channel characteristics, there are still some deficiencies in the description of the exit channel. In such a region a linear van der Waals well produces a rich long-lived resonance pattern that is very sensitive to fine details of the PES. Such resonance complexes decay preferentially into the $v'=3$ product channel, giving sharp peaks in the integral and differential cross sections, which may presumably have been experimentally averaged to give broad features. This result together with other experimental evidence of finer observable details not presented here, shows that the description of the van der Waals exit channel has to be improved in order to establish the importance of such states, even though there are some evidence that nonadiabatic effects also play a role on the resonance mechanism.[36,37]

However, the potential energy surfaces used so far miss the correct reaction exothermicity. Recently a large effort[38–40] has been spent to produce further *ab initio* ground potential energy surfaces with the aim of solving this problem. In particular, a new set of *ab initio* points[40] has generated a surface that led to a large increase of the $v'=3$ HF production, in the direction required by the experiments. However, the classical barrier height obtained in that work (about 101 meV) is considerably larger than the one used in this work and in Ref. 3 (about 68 meV) so that it will be

TABLE III. Comparison between theoretical rate constants for SW and PES III (in cm^3 $molecule^{-1}$ s^{-1} $\times 10^{-12}$) for the F+HD→HF(DF)+D(H) reaction as a function of temperature.

	k_{HF+D}			k_{DF+H}		
T (K)	PES III[a]	SW[a]	SW[b]	PES III[a]	SW[a]	SW[b]
100	1.22	2.87	2.71	0.28	0.43	0.44
120	1.81	3.64	3.54	0.58	0.76	0.76
140	2.51	4.43	4.39	0.90	1.19	1.19
160	3.33	5.26	5.29	1.51	1.73	1.74
180	4.25	6.14	6.22	2.13	2.36	2.37
200	5.24	7.07	7.20	2.82	3.06	3.07
220	6.28	8.03	8.22	3.58	3.82	3.83
240	7.36	9.01	9.27	4.37	4.63	4.63
260	8.46	10.0	10.3	5.12	5.46	5.46
280	9.56	11.0	11.4	6.04	6.31	6.31
300	10.6	12.0	12.5	6.90	7.17	7.17

[a]Present work.
[b]Reference 12.

interesting to test such a surface with the cross sections and rate constant data that we have successfully interpreted in this paper and in Ref. 3 with PES III. The time independent dynamical calculations presented in this work generated for the first time the complete **S** matrix, including all open entrance and exit channels at the given energy, for a reaction having three different atoms: this will permit the full analysis of the microscopic steric effect by the stereodirected representation (as we did in Ref. 34 for $F+H_2$), as well as a detailed resonance analysis as a function of J by the exact (lifetime) **Q** matrix, also generated by our code.[10,32] This will allow us to get further insight on the reaction mechanism—particularly on the effect of the attack angle, which is conjectured in Sec. III A to cooperate with tunneling to establish the essential features of the observed kinetic isotope effect, and on the role of the exit channel long lived states, which provide the rich resonance pattern exhibited by this reaction. Furthermore, complete **S** matrix results will be employed for the theoretical interpretation of existing experimental information on state-to-state integral and differential cross sections.[8,9]

ACKNOWLEDGMENTS

We are grateful to K. Liu (Taipei) for sending us the original data of his work. M. Sevryuk (Moscow) and T. V. Tscherbul (Vancouver) are also kindly acknowledged for stimulating discussions. This work was supported by the Italian Ministero dell'Istruzione, dell'Universitá e della Ricerca (MIUR) through PRIN and FIRB contracts, the Spanish Ministry of Science and Education, Project No. CTQ2004-01102, and HPC-Europa Transnational Access programme (Contract no. HPRI-1999-CT00071) in relation to the Access to CESCA and CEPBA Large Scale Facilities.

[1] D. M. Neumark, A. M. Wodtke, G. N. Robinson, C. C. Hayden, and Y. T. Lee, J. Chem. Phys. **82**, 3045 (1985).
[2] See, e.g., S. C. Althorpe and D. C. Clary, Annu. Rev. Phys. Chem. **54**, 493 (2003).
[3] V. Aquilanti, S. Cavalli, D. De Fazio, A. Volpi, A. Aguilar, and J. M. Lucas, Chem. Phys. **308**, 237 (2005); Chem. Phys. Lett. **371**, 504 (2003).
[4] D. M. Neumark, A. M. Wodtke, G. N. Robinson, C. C. Hayden, R. Schobatake, R. K. Sparks, T. P. Schaefer, and Y. T. Lee, J. Chem. Phys. **82**, 3067 (1985).
[5] J. F. Castillo and D. E. Manolopoulos, Faraday Discuss. **110**, 119 (1998).
[6] R. T. Skodje, D. Skouteris, D. E. Manolopoulos, S.-H. Lee, F. Dong, and K. Liu, J. Chem. Phys. **112**, 4536 (2000); Phys. Rev. Lett. **85**, 1206 (2000).
[7] K. Stark and H.-J. Werner, J. Chem. Phys. **104**, 6515 (1996).
[8] S.-H. Lee, F. Dong, and K. Liu, J. Chem. Phys. **116**, 7839 (2002).
[9] W. W. Harper, S. A. Nizkorodov, and D. Nesbitt, J. Chem. Phys. **116**, 5622 (2002).
[10] V. Aquilanti, S. Cavalli, D. De Fazio, A. Simoni, and T. V. Tscherbul, J. Chem. Phys. **123**, 50134 (2005).
[11] V. Zeman, M. Shapiro, and P. Brumer, Phys. Rev. Lett. **92**, 133204 (2004).
[12] D. H. Zhang, S.-Y. Lee, and M. Baer, J. Chem. Phys. **112**, 9802 (2000).
[13] B. Hartke and H.-J. Werner, Chem. Phys. Lett. **280**, 430 (1997).
[14] M. H. Alexander, D. E. Manolopoulos, and H.-J. Werner, J. Chem. Phys. **113**, 11084 (2000).
[15] T.-X. Xie, Y. Zhang, and K.-L. Han, Chem. Phys. Lett. **398**, 313 (2004).
[16] Y. Zhang, T.-X. Xie, K.-L. Han, and J. Z. H. Zhang, J. Chem. Phys. **120**, 6000 (2004).
[17] Y.-R. Tzeng and M. H. Alexander, J. Chem. Phys. **121**, 5183 (2004).
[18] V. Aquilanti, S. Cavalli, D. De Fazio, A. Volpi, A. Aguilar, X. Gimenez, and J. M. Lucas, Phys. Chem. Chem. Phys. **4**, 401 (2002).
[19] V. Aquilanti, S. Cavalli, F. Pirani, A. Volpi, and D. Cappelletti, J. Phys. Chem. **105**, 2401 (2001).
[20] V. Aquilanti, R. Candori, D. Cappelletti, E. Luzzatti, and F. Pirani, Chem. Phys. **145**, 293 (1990).
[21] A. Persky and H. Kornweitz, Int. J. Chem. Kinet. **29**, 67 (1997).
[22] A. Persky, Chem. Phys. Lett. **401**, 455 (2005).
[23] V. Aquilanti, S. Cavalli, and D. De Fazio, J. Chem. Phys. **109**, 3792 (1998).
[24] V. Aquilanti, S. Cavalli, D. De Fazio, A. Volpi, A. Aguilar, X. Gimenez, and J. M. Lucas, J. Chem. Phys. **109**, 3805 (1998).
[25] V. Aquilanti, G. Capecchi, S. Cavalli, D. De Fazio, P. Palmieri, C. Puzzarini, A. Aguilar, X. Giménez, and J. M. Lucas, Chem. Phys. Lett. **318**, 619 (2000); Mol. Phys. **98**, 1835 (2000).
[26] V. Aquilanti, S. Cavalli, and D. De Fazio, J. Phys. Chem. **99**, 15694 (1995); D. De Fazio, V. Aquilanti, and S. Cavalli, Int. J. Quantum Chem. **93**, 91 (2003).
[27] V. Aquilanti, S. Cavalli, D. De Fazio, A. Volpi, A. Aguilar, X. Gimenez, and J. M. Lucas, Phys. Chem. Chem. Phys. **1**, 1091 (1999).
[28] D. Skouteris, J. F. Castillo, and D. E. Manolopoulos, Comput. Phys. Commun. **133**, 128 (2000).
[29] A. Persky and H. Kornweitz, J. Phys. Chem. A **108**, 8599 (2004).
[30] See http://www.chm.unipg.it/chimgen/mb/theo2/home/pagine/ricerca
[31] J. M. Bowman, Chem. Phys. **308**, 255 (2005).
[32] V. Aquilanti, S. Cavalli, A. Simoni, A. Aguilar, J. M. Lucas, and D. De Fazio, J. Chem. Phys. **121**, 11675 (2004).
[33] J. T. Muckerman, J. Chem. Phys. **54**, 1155 (1971); G. W. Johnston, H. Kornweitz, I. Schechter, A. Persky, B. Katz, R. Bersohn, and R. D. Levine, J. Chem. Phys. **94**, 2749 (1991).
[34] J. Aldegunde, J. M. Alvarino, D. De Fazio, S. Cavalli, G. Grossi, and V. Aquilanti, Chem. Phys. **304**, 251 (2004).
[35] F. Dong, S.-H. Lee, and K. Liu, J. Chem. Phys. **113**, 3633 (2000).
[36] S.-H. Lee, F. Dong, and K. Liu, Faraday Discuss. **127**, 49 (2004).
[37] Y.-R. Tzeng and M. H. Alexander, Phys. Chem. Chem. Phys. **6**, 5018 (2004).
[38] M. Hayes, M. Gustafsson, A. M. Mebel, and R. T. Skodje, Chem. Phys. **308**, 259 (2005).
[39] W. Cardoen, R. Gdanitz, and J. Simons, J. Phys. Chem. A **110**, 564 (2006).
[40] M. Qiu, Z. Ren, L. Chi *et al.*, Science **311**, 1440 (2006).